Industrial Engineering Journal
ISSN: 0970-2555
Volume : 54, Issue 5, No.4, May : 2025

THERMAL STRESS ANALYSIS AND CUTTING PARAMETERS OPTIMIZATION IN ALUMINIUM 6061 T6 ALLOY MACHINING PROCESS

Mr. Muhammed Shameem T S, PG Student, Department of Mechanical Engineering, NSS College of Engineering, Palakkad, Kerala, India.
Dr. Jyothi Sankar P R, Professor, Department of Mechanical Engineering, NSS College of Engineering, Palakkad, Kerala, India.

ABSTRACT
This research is concerned with the analysis of thermal stress in the aluminium 6061 T6 workpiece during turning operations using ANSYS Workbench to simulate and forecast thermal behaviour. The aim is to avoid distortion, improve surface finish, and increase tool life. A regression model will also be created using STATGRAPHICS Centurion to forecast important parameters like cutting temperature, equivalent stress, and maximum shear stress. This will offer an understanding of how cutting parameters and thermal stress are related. In order to maximize the machining process, MATLAB will be utilized in finding an optimum level of cutting speed, feed rate, depth of cut, and rake angle that will result in an effective material removal rate along with a reduction of thermal stress. Through the combination of simulation and optimization techniques, this research aims to increase machining effectiveness, enhance product quality, and extend tool lifespan, providing a sustainable method for material removal in manufacturing operations.

Keywords:
Thermal stress, Aluminium 6061-T6, Turning operations, ANSYS Workbench, STATGRAPHICS Centurion, Regression model, Cutting temperature, Equivalent stress, Maximum shear stress, MATLAB, Optimization.

I. Introduction
In modern manufacturing industries, the demand for producing high-quality components with precision, efficiency, and sustainability is more critical than ever. Among various metalworking processes, turning remains a key subtractive machining operation widely used across sectors. As industries strive for enhanced productivity and tighter tolerances, understanding thermal behavior during turning has become essential due to its influence on surface finish, dimensional accuracy, tool wear, and overall process stability. This research investigates the thermal stress behavior during the turning of Aluminum 6061-T6, an age-hardened alloy extensively used in aerospace, automotive, and structural applications due to its excellent strength-to-weight ratio, corrosion resistance, and machinability. However, its heat sensitivity poses challenges during machining, often resulting in thermal distortion, increased tool wear, and compromised surface integrity. To address these challenges, a comprehensive approach is adopted that combines simulation, statistical modeling, and optimization. ANSYS Workbench is used to simulate the thermal and mechanical responses during turning through Finite Element Analysis (FEA), enabling detailed evaluation of temperature distribution, stress concentration, and deformation. STATGRAPHICS Centurion is employed to develop regression models that relate key output parameters, such as cutting temperature, von Mises stress, and maximum shear stress, to machining variables like cutting speed, feed rate, depth of cut, and rake angle. Further, MATLAB-based multi-objective optimization is conducted to identify the optimal combination of parameters that maximizes material removal rate (MRR) while minimizing thermal stress and tool degradation. This integrated methodology aims to improve machining effectiveness, enhance surface quality, extend tool life, and promote sustainable manufacturing practices in high-performance environments.

II. Literature Review

Thermal stress analysis during machining, especially in turning operations, has emerged as a critical area of study due to its significant impact on product quality and tool longevity. The primary source of thermal stress is the intense heat generated by plastic deformation and friction at the tool–workpiece interface. This localized heating can lead to structural distortions, reduced mechanical properties, and compromised dimensional accuracy in the final product [1]. To address this, researchers have increasingly adopted Finite Element Analysis (FEA) tools such as ANSYS Workbench, which enable detailed simulation of thermal and mechanical interactions under varied machining conditions [2].
Aluminum 6061-T6 is a widely utilized material in sectors such as aerospace and automotive due to its excellent strength-to-weight ratio, corrosion resistance, and good machinability. However, it remains thermally sensitive during machining. Excessive heat can induce residual stresses, thermal softening, and dimensional inaccuracies, while also accelerating the formation of built-up edge (BUE) and tool wear [3]. Understanding and mitigating these effects through thermal stress analysis is essential for maintaining the structural integrity and performance of machined components. Studies using FEA have shown that optimizing parameters such as cutting speed, feed rate, and depth of cut can significantly reduce thermal stress and its detrimental consequences [4].
Beyond simulation, statistical and empirical modeling techniques play a crucial role in establishing relationships between machining inputs and performance outputs. Regression analysis, particularly through software like STATGRAPHICS Centurion, allows for the prediction of outcomes such as cutting temperature, von Mises stress, and maximum shear stress based on process parameters. These models enable sensitivity analysis and support informed decision-making for process improvement, making them valuable tools in precision machining of Aluminum 6061-T6 [5].
Optimization of machining parameters is another vital aspect of enhancing efficiency and sustainability in manufacturing. Computational platforms like MATLAB are commonly used to solve multi-objective optimization problems using algorithms such as genetic algorithms (GA), particle swarm optimization (PSO), and gradient-based methods. These techniques help identify the optimal combination of cutting parameters that maximize productivity (e.g., material removal rate) while minimizing adverse effects like thermal stress and tool wear [6]. When combined with simulation and regression models, these optimization strategies lead to robust process designs that improve both technical performance and operational cost-effectiveness [7].
Tool wear, closely linked to thermal conditions at the cutting interface, remains a major challenge in turning operations. High temperatures can degrade tool material properties, causing flank wear, crater wear, and even catastrophic failure. For aluminum alloys, which have high thermal conductivity and adhesive tendencies, built-up edge formation is a common issue. This alters the effective geometry of the cutting edge, negatively impacting surface finish and dimensional accuracy [8]. Thus, managing cutting temperature is essential for controlling wear mechanisms and extending tool life.
Surface finish, another key quality metric, is heavily influenced by thermal effects during machining. Elevated temperatures can cause thermal expansion in the tool and workpiece, leading to variations in tool path and increased surface roughness. This is especially critical in industries like aerospace where surface integrity directly affects fatigue resistance and part reliability. Studies have shown that maintaining optimal cutting temperatures is essential to achieving high-quality surface finishes [9].
The evolution of thermal modeling has been significantly accelerated by the advancement of computational methods. Early analytical models were limited in scope, but modern FEA-based simulations now allow for realistic modeling of transient heat transfer, stress distribution, and deformation. Tools like ANSYS Workbench enable simulations under various cutting environments—dry, wet, and minimum quantity lubrication (MQL)—providing insights into how cooling and lubrication influence thermal gradients and stress concentrations [10]. These insights are vital for developing sustainable machining processes with reduced coolant usage and improved energy efficiency.
The integration of regression modeling, FEA, and optimization reflects a shift toward intelligent and adaptive manufacturing systems aligned with Industry 4.0 principles. Researchers now use these

combined tools to develop predictive, data-driven machining strategies. This integration supports real-time decision-making, predictive maintenance, and zero-defect manufacturing, as highlighted in recent literature from sources such as the CIRP Journal of Manufacturing Science and Technology [11]. Such approaches enhance process reliability, repeatability, and responsiveness to variable manufacturing conditions [12].

Sustainability has become a central theme in contemporary machining research. Optimizing cutting parameters to manage thermal stress not only improves product quality but also reduces energy consumption and tool replacement frequency. This leads to less material waste, fewer rejected parts, and lower overall manufacturing costs. Studies report that simulation-based optimization, combined with statistical modeling, can achieve up to 25% energy savings in machining operations, reinforcing the environmental and economic value of integrated approaches [13].

III. Methodology

The present work employs a hybrid approach of finite element simulation, statistical modelling, and optimization to explore the thermal stress response of Aluminium 6061-T6 during orthogonal turning operations. The aim is to enhance machining performance in terms of minimized thermally induced distortions, enhanced surface integrity, and enabling sustainable manufacturing. The methodology is carried out in various stages, briefly described below.

3.1 Machining Setup and Process Definition

Orthogonal cutting was selected as the machining mode within this study. In this idealized turning mode, the cutting edge of the tool remains perpendicular to the cutting velocity direction, simplifying the analysis of temperature and stresses into a two-dimensional space. Such a setup permits simpler interpretation of thermal and mechanical occurrences as opposed to oblique cutting. The orthogonal condition was achieved by minimizing the tool nose radius and employing a straight cutting edge, thereby ensuring controlled experimentation and increased accuracy in simulation.

The workpiece material used is Aluminium 6061-T6, a precipitation-hardenable alloy used extensively in the aerospace, automotive, and structural industries. It has a very good strength-to-weight ratio, good thermal conductivity, and machinability.

The principal material properties (Table 3.1) including Young's modulus, Poisson's ratio, shear modulus, and thermal conductivity were input into the simulation environment to accurately describe the material behaviour.

Table 3.1. Material properties of Aluminium 6061-T6

Property	**Value (unit)**
Density	2703 (kg/m^3)
Youngs modulus	6.904e+10 (Pa)
Poisons ratio	0.33
Bulk modulus	6.786e+10 (Pa)
Shear modulus	2.5955e+10 (Pa)
Isotropic secant coefficient of thermal expansion	2.278e-05 (1/^{0}C)
Tensile ultimate strength	3.131e+08 (Pa)
Tensile yield strength	2.592e+08 (Pa)
Isotropic thermal conductivity	155.3 (W/m^{0}C)
Specific heat constant pressure	915.7 (J/kg^{0}C)

A single-point tungsten carbide insert was used due to its high hardness, thermal resistance, and favourable interaction with aluminium. Key properties of the tool material are summarized in Table 3.2.

Table 3.2. Material properties of tungsten carbide

Property	Value (unit)
Density	20 (kg/m^3)
Youngs modulus	6e^{11}(Pa)
Poisons ratio	0.2
Bulk modulus	3.33e^{11}(Pa)
Shear modulus	2.5e^{11}(Pa)
Specific heat	1.84e^{-7}(J/kg)

In machining operations, the selection and variation of cutting parameters significantly influence thermal and mechanical responses, particularly in high-speed turning of aluminium alloys. For this investigation, three key process parameters were identified and systematically varied: cutting speed (v), depth of cut (d), and rake angle (α). These parameters were chosen based on their direct impact on chip formation, heat generation, and stress distribution in the workpiece.in this experiment cutting parameters values taken as Cutting Speed (v): 50 m/min, 150 m/min, and 250 m/min. Depth of Cut (d): 0.1 mm, 0.2 mm, and 0.5 mm .Rake Angle (α): –6°, 0°, and +15° .The chosen levels cover a realistic and practical range for machining Aluminium 6061-T6, considering both conventional and high-speed cutting regimes.

To evaluate the thermal and mechanical behavior of the workpiece during orthogonal turning, three key response variables are considered: cutting temperature, maximum shear stress, and equivalent (von Mises) stress. These outputs are critical for assessing machining performance, thermal effects, and structural integrity of the workpiece and tool. Cutting temperature reflects the peak thermal load at the tool–workpiece interface, primarily arising from plastic deformation in the shear zones and friction at the chip-tool contact. It significantly influences thermal stress, tool wear, surface integrity, and dimensional accuracy, making it a vital parameter for thermal analysis and process optimization. Maximum shear stress represents the highest shear force within the material during chip formation and is directly tied to the mechanics of deformation. Elevated shear stresses can lead to microstructural damage, reduced fatigue life, and increased thermal–mechanical interaction, especially when coupled with high temperatures. Von Mises stress, a yield-based scalar measure of combined stresses, is employed to evaluate the onset of plastic deformation under complex loading. It offers a comprehensive understanding of stress concentration zones and potential failure locations, thereby ensuring the workpiece's structural integrity during machining.

3.2 Modelling and Simulation

To accurately predict the thermal stress behaviour of Aluminium 6061-T6 during orthogonal turning operations, finite element simulation (FEM) is conducted using ANSYS Workbench. The simulation aims to replicate realistic machining conditions by modelling the material removal process, heat generation, and resulting thermal and mechanical responses of the workpiece. The structured simulation workflow includes the following major steps:

A 3D model of the workpiece and tool is created to represent the orthogonal cutting scenario. A rectangular domain is designed with dimensions large enough to capture the deformation and thermal effects without boundary interference. The cutting tool, made of tungsten carbide, is modelled as a rigid body due to its significantly higher hardness compared to aluminium. The tool has a specified rake angle (positive, neutral, or negative) based on the experimental setup. A small clearance angle is also provided to prevent tool rubbing. The workpiece has a length of 50mm, height 10 mm and 4mm thickness. The tungsten carbide cutting tool have width of cut 4mm.in this the rake angles of cutting tool taken as positive, negative and zero values are 15^0,-6^0 and 0^0 respectively.

Industrial Engineering Journal
ISSN: 0970-2555
Volume : 54, Issue 5, No.4, May : 2025

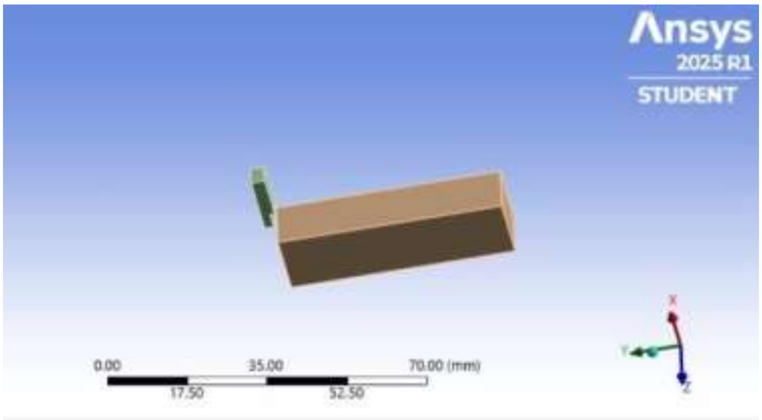

Figure 3.1. 3D model of workpiece and tool

A refined mesh is applied near the tool-workpiece interface where intense thermal and mechanical gradients are expected (primary shear zone and chip-tool interface).Coarser mesh is used farther away from the contact region to reduce computational cost without sacrificing accuracy. Element Type is Quadrilateral elements with thermal–mechanical coupling capability are used to ensure simultaneous analysis of stress and temperature fields. Mesh Independence Study Conducted to ensure that the simulation results are not significantly affected by further mesh refinement. the number of nodes is 85000.thus the mesh was found to be independent at fine level. Details of body sizing is that the model meshed with element size of 1.5251 mm.

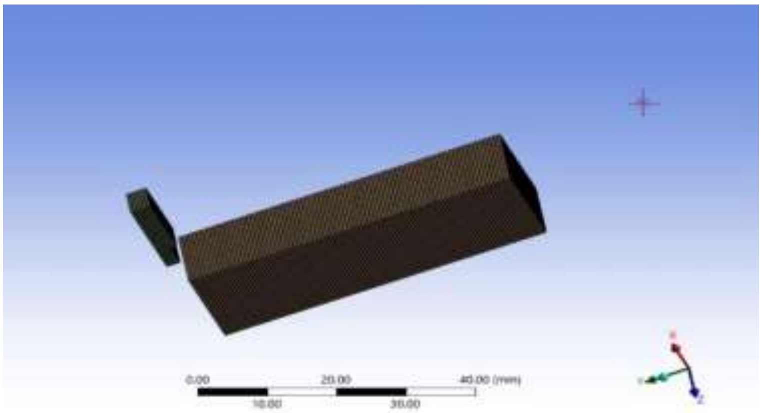

Figure 3.2. Meshed image of model

After completing the pre-processing steps (geometry setup, meshing, material assignment, boundary conditions, and displacement components), the simulation is executed in ANSYS Workbench. The model is solved as a coupled thermo-mechanical analysis, allowing for the simultaneous evaluation of: Temperature distribution, Equivalent (Von Mises) stress distribution, Maximum shear stress fields. The temperature distribution will take as output from the transient thermal analysis while it has the same procedure as of explicit dynamics. Multiple simulations are performed by varying cutting parameters: Cutting Speed (depth of Cut (d),Rake Angle (α).From each simulation run, the following outputs are extracted: Peak Cutting Temperature: Measured at the tool–workpiece interface or near the primary shear zone. Maximum Shear Stress: Captured from the shear stress contours within the workpiece. Equivalent (Von Mises) Stress: Recorded across the deformation zone to assess yielding tendencies. Results are compiled and organized systematically to serve as inputs for the subsequent statistical regression modelling using STATGRAPHICS Centurion. Visualization techniques such as contour plots, vector plots, and temperature distribution maps are used to interpret the results and validate physical behaviour.

Total Deformation

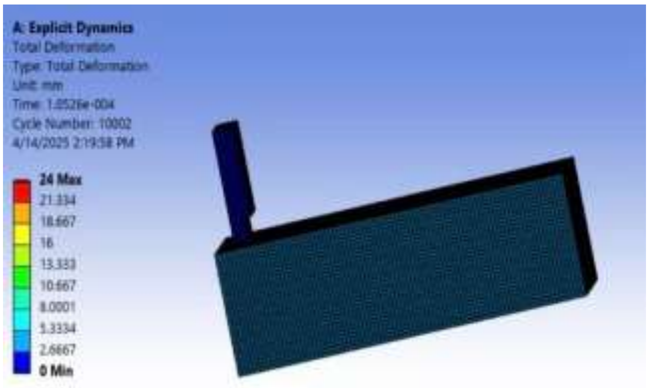

Figure 3.3. Starting of elastic deformation

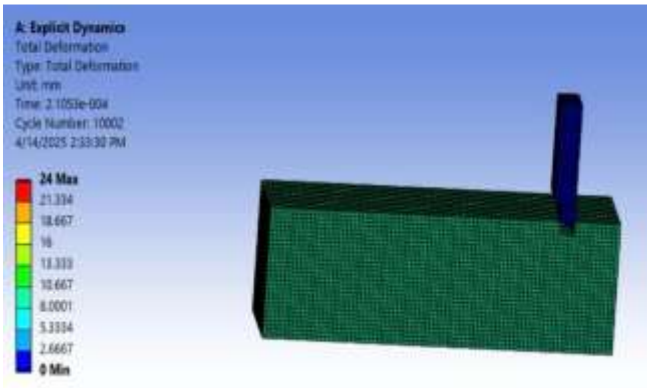

Figure 3.4. Plastic deformation growth.

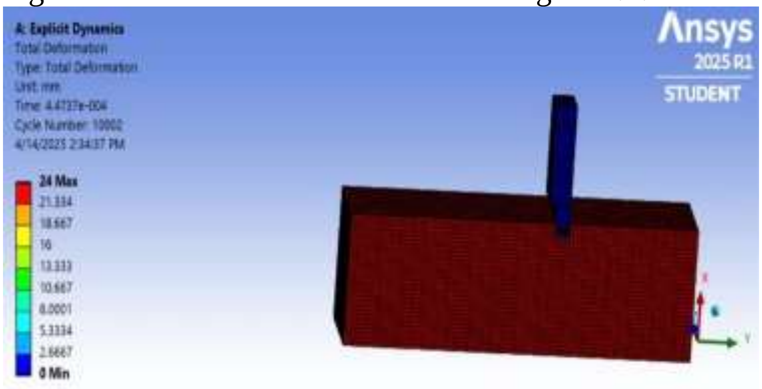

Figure 3.5. Full plastic deformation

Figure 3.3 illustrates the Early Stage of Cutting. at time 1.0526e-004 seconds**,** the tool has initiated contact with the workpiece. Deformation is localized at the immediate vicinity of the tool tip, indicating the onset of elastic deformation. The maximum deformation value recorded at this stage is approximately 24 mm**.** The deformation distribution is confined to a small region, with minimal propagation into the surrounding material. This stage reflects the initial mechanical response of the workpiece material to the tool's applied displacement before significant plastic deformation occurs.

Figure 3.4 shows the Intermediate Stage of Cutting at 2.1053e-004 seconds**,** the cutting tool has penetrated deeper into the workpiece. The deformation zone extends further from the tool, demonstrating a transition from elastic to plastic behaviour. The stress concentration near the cutting zone increases, leading to greater material displacement in front of the tool. The maximum deformation remains around 24 mm**,** but the area affected by substantial deformation expands significantly. This stage signifies the development of a shear zone where plastic flow dominates the material response. It marks the beginning of chip formation.

Figure 3.5 shows the Advanced Stage of Cutting at a later time, 4.4378e-004 seconds**,** the deformation has propagated widely throughout the workpiece. The red regions in the deformation contour plot indicate the highest strain concentration directly under and behind the tool. Deformation is no longer localized but spreads significantly, with a large volume of the material undergoing substantial plastic deformation. Again, the maximum deformation remains close to 24 mm.at this stage, the material experiences significant plastic flow and chip separation begins to occur, which is consistent with actual machining behaviour. This mature stage of deformation confirms the effectiveness of the applied boundary conditions, loading parameters, and meshing strategy.

Maximum Shear Stress

Industrial Engineering Journal
ISSN: 0970-2555
Volume : 54, Issue 5, No.4, May : 2025

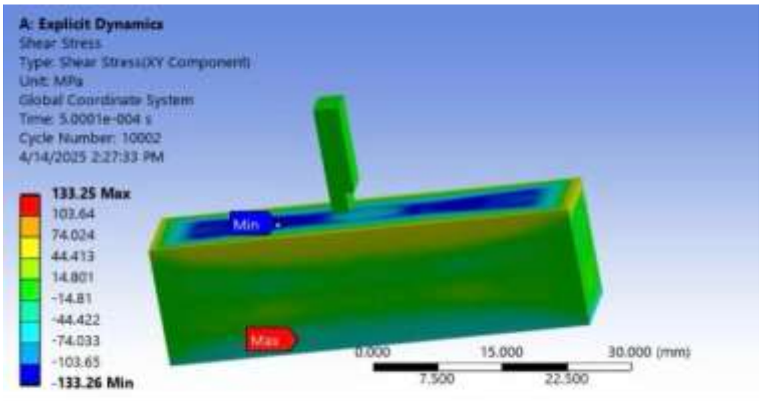

Figure 3.6. Shear stress distribution with concentrated stress near tool edge, moderate loading

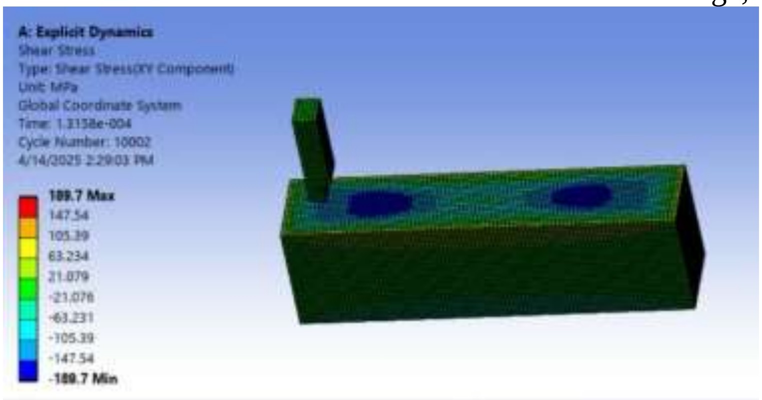

Figure 3.7. Shear stress distribution with higher concentrated stress zones, more aggressive cut

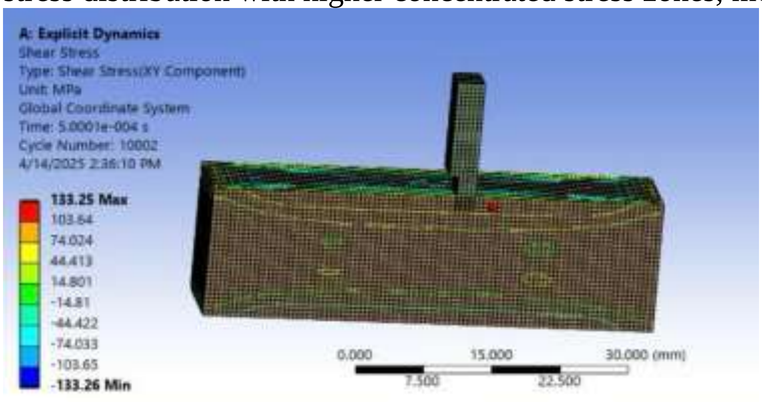

Figure 3.8. Shear stress distribution with wider distribution of stresses, stable cutting

Figure 3.6 shows the shear stress distribution on the workpiece subjected to machining action. Maximum Shear Stress is 133.25 MPa and Minimum Shear Stress is -133.26 MPa. Observations are, High stress concentrations are observed at the tool-workpiece interface, indicating the area where maximum material shearing occurs. The stress is symmetrically distributed along the contact region, with intense positive (red) and negative (blue) shear stresses localized around the tool tip. Away from the immediate cutting zone, the material experiences significantly lower stress magnitudes. Interpretations are The results suggest that the primary shear zone is confined near the cutting edge, as expected in high-speed cutting operations. The stress pattern indicates potential regions prone to material removal, chip formation, or plastic deformation.

Figure 3.7 illustrates another simulation scenario of shear where different boundary or tool displacement conditions were applied. Maximum Shear Stress is 189.7 MPa, Minimum Shear Stress: -189.7 MPa. Observations are, A noticeable increase in the maximum shear stress compared to the first case is evident. Two distinct high-stress zones appear beneath the tool, suggesting a more aggressive cutting interaction. The stress distribution is more concentrated and localized, with sharper

Industrial Engineering Journal
ISSN: 0970-2555
Volume : 54, Issue 5, No.4, May : 2025
gradients around the cutting area. Interpretation is, significant increase in maximum shear stress points to higher material resistance and cutting forces. This condition likely represents either a deeper cut or higher tool velocity, resulting in more intense mechanical loading. Such stress conditions could lead to faster tool wear or material fracture if sustained.
Figure 3.8 represents another simulation setup with Maximum Shear Stress: 133.25 MPa and Minimum Shear Stress: -133.26 MPa. Observations are ,The stress distribution appears more spread across a larger volume of the workpiece compared to previous cases. The peak stresses are still located at the cutting interface but extend more uniformly across the surface and subsurface layers. Moderate stress values dominate, with lower intensity gradients compared to the second simulation case. Interpretations are, This pattern indicates a less aggressive cutting condition, possibly with a lower feed rate or reduced tool penetration. The broader stress distribution suggests that the workpiece is undergoing general deformation rather than localized failure. Such cutting conditions might be favourable for improving surface finish and reducing the risk of cracks or premature material failure.

Temperature

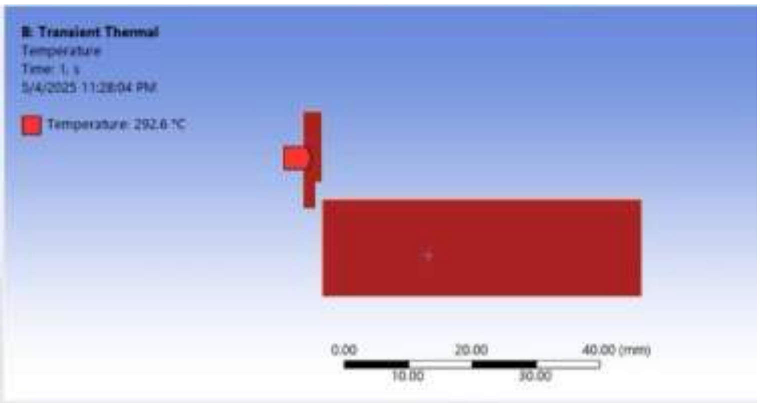

Figure 3.9. Transient thermal temperature distribution 1

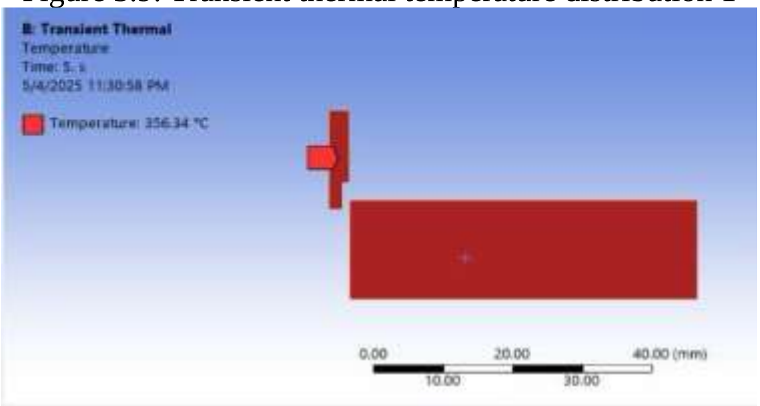

Fig 3.10. Transient thermal temperature distribution 2

Fig 3.9 shows the initial time step of 1 second, the temperature distribution on the workpiece shows a relatively lower peak temperature of approximately 292.6 °C. This corresponds to a rake angle of 15°, a low cutting speed of 50 m/min, and a shallow depth of cut (0.1 mm). These conditions represent a conservative and less aggressive machining environment. In this stage: Heat generation is minimal due to reduced friction and lower deformation rates. The tool-workpiece interface shows localized heating, suggesting that the majority of the energy is being consumed in overcoming the initial material resistance. The thermal load is manageable, which implies lower thermal stress but slower material removal.
In Fig 3.10, the final simulation time of 2 seconds, the temperature profile remains steady at 356.34 °C, indicating that the system has likely reached a thermal steady-state. The cutting parameters remain the same as in Figure 2.Detailed interpretation is that The temperature plateau suggests that the material is undergoing consistent plastic deformation under stable thermal conditions. The heat concentration

Industrial Engineering Journal
ISSN: 0970-2555
Volume : 54, Issue 5, No.4, May : 2025

remains near the cutting edge, with some conduction into the bulk material, which is a typical behaviour in dry machining of aluminium alloys. This temperature is within acceptable limits for Aluminium 6061-T6, ensuring good machinability without reaching softening or melting points.

Von Mises Equivalent Stress

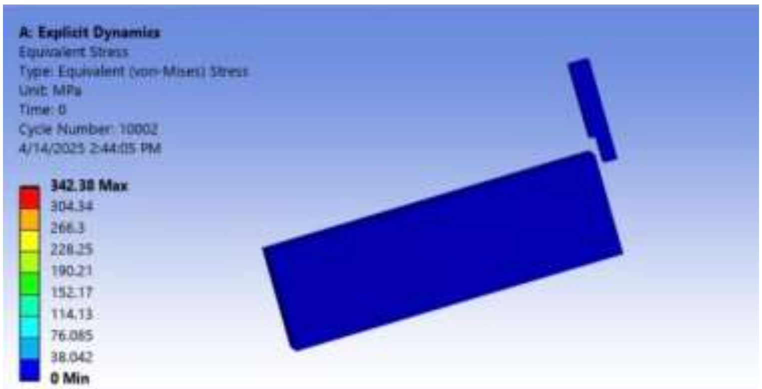

Figure 3.11. Initial equivalent (Von-Mises) stress distribution at time zero

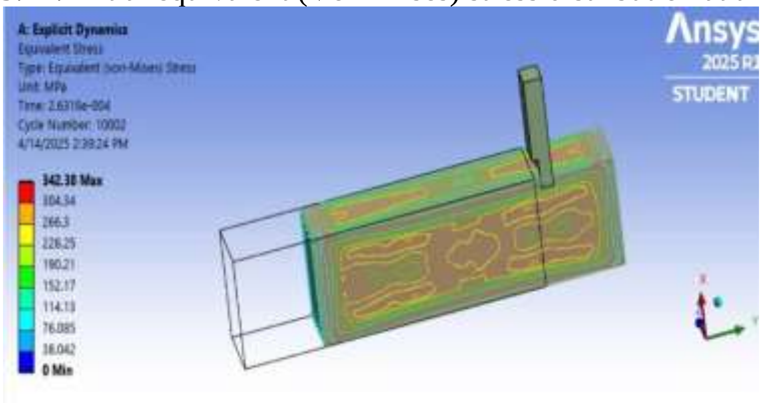

Figure 3.12. Equivalent (Von-Mises) stress contours during cutting initiation

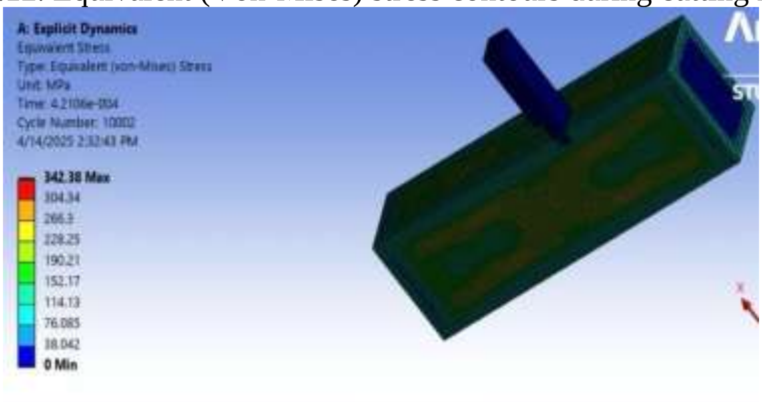

Figure 3.13. Equivalent (Von-Mises) stress distribution at intermediate cutting stage

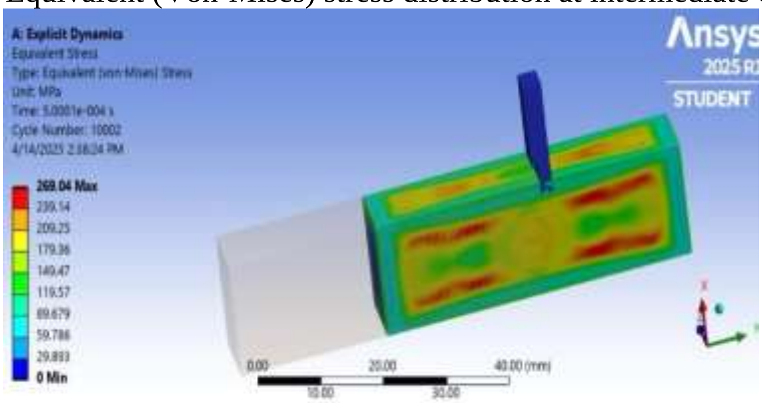

Industrial Engineering Journal
ISSN: 0970-2555
Volume : 54, Issue 5, No.4, May : 2025

Figure 3.14. Equivalent (Von-Mises) stress field during material removal

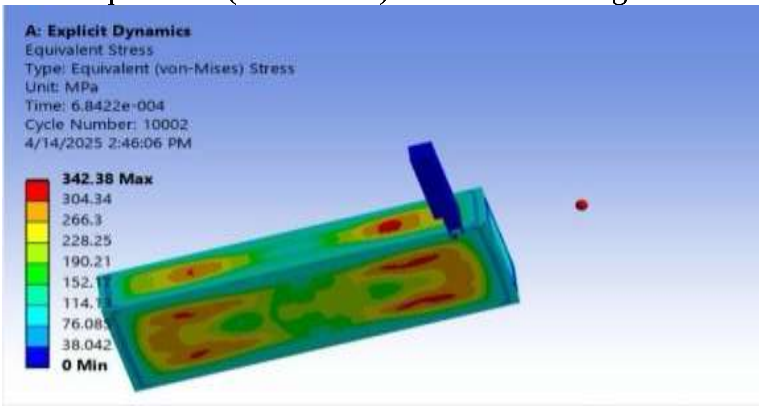

Figure 3.15. Final equivalent (Von-Mises) stress distribution after cutting progression

Figure 3.11 shows the Initial Equivalent (Von-Mises) Stress Distribution at Time Zero. This figure shows the initial state of the simulation where the equivalent von-Mises stress is calculated at time = 0 seconds. At this point, no external loading has yet been applied. The figure displays minimal to zero stress throughout the tool and workpiece, confirming that initial conditions are properly set. The colour scale ranges from 0 MPa to 342.38 MPa, but actual stresses are close to zero. Significance is Serves as a baseline for stress development once loading and deformation begin.

Figure 3.12 illustrates the Equivalent (Von-Mises) Stress Contours during Cutting Initiation. This figure illustrates the distribution of equivalent stress at an early deformation stage, using a contour (line) plot over the meshed body. Significant stress concentrations start appearing around the tool-workpiece interaction area. The highest stress regions are close to the cutting edge of the tool, indicating localized plastic deformation. Significance is Indicates where the material begins to yield first under the tool force.

Figure 3.13 shows the Equivalent (Von-Mises) Stress Distribution at Intermediate Cutting Stage. a further advanced simulation time, the workpiece shows broader areas affected by stresses. The stress field is expanding from the cutting zone into the bulk of the workpiece, with stress values growing significantly around the cutting tip. The maximum value again approaches 342.38 MPa. Significance is that Reflects the propagation of plastic deformation deeper into the workpiece during the cutting process.

Figure 3.14 illustrates the Equivalent (Von-Mises) Stress Field during Material Removal. This figure captures the stress distribution once a significant portion of the material is removed. The scale slightly differs here (Max 269.04 MPa), likely due to a change in cutting parameters or material response. The region ahead of the tool shows compressive stresses, while tensile stresses are found behind the tool, typical in metal cutting processes. Significance is that Shows how stresses are redistributed in the material during chip formation and removal.

Figure 3.15 shows Final Equivalent (von-Mises) Stress Distribution After Cutting Progression This final figure shows a more stabilized stress pattern across the workpiece after extended deformation. The equivalent stress remains high around the tool's cutting path, indicating areas where the material has undergone the most plastic strain. The stress distribution is more symmetric and uniform compared to earlier stages. Significance is that Important for analysing residual stresses and understanding long-term material performance after machining.

Temperature, Maximum Shear Stress and Von Mises Equivalent Stress Distribution

Table 3.3. Distribution of temperature according to the cutting speed, depth of cut and rake angle

α	15^0			0^0			-6^0		
V(m/min)	50	150	250	50	150	250	50	150	250
$T_{d=0.1}$	292.96	299.01	308.79	344.57	356.34	365.84	372.14	381.26	393.75
$T_{d=0.2}$	268.51	279.68	292.12	381.96	396.56	412.13	425.12	431.89	452.40

$T_{d=0.5}$	287.76	298.75	317.43	326.48	335.92	351.64	354.57	356.80	361.12

Table 3.4. Distribution of maximum shear stress according to the cutting speed, depth of cut and rake angle

α	15^0			0^0			-6^0		
V (m/min)	50	150	250	50	150	250	50	150	250
$\tau_{d=0.1}$	133.25	138.85	139.64	158.86	159.05	159.62	164.62	167.31	169.79
$\tau_{d=0.2}$	114.58	127.42	135.74	169.90	172.78	180.91	187.81	187.95	193.23
$\tau_{d=0.5}$	139.10	142.65	153.01	166.86	178.43	189.7	190.39	191.86	195.29

Table 3.5. Distribution of Von Mises equivalent stress according to cutting speed, depth of cut and rake angle

α	15^0			0^0			-6^0		
V(m/min)	50	150	250	50	150	250	50	150	250
$\sigma_{d=0.1}$	342.38	347.26	356.01	374.54	381.83	382.19	391.08	393.62	393.24
$\sigma_{d=0.2}$	269.04	281.04	295.32	341.57	342.38	349.04	357.96	369.73	378.91
$\sigma_{d=0.5}$	342.97	361.63	374.16	380.18	384.53	391.46	392.24	392.69	394.58

Where V is the cutting speed, d is the depth of cut, α is the rake angle. and T, τ, σ are the temperature in degree Celsius, shear stress in MPa and equivalent stress in MPa respectively.

From table 3.3 we have to know at a constant depth of cut and rake angle, the maximum temperature generally increased with increasing cutting speed. For instance, at α = 15° and Td = 0.1 mm, the temperature rose from 292.96°C at 50 m/min to 308.79°C at 250 m/min. This behaviour is attributed to higher plastic deformation rates at higher speeds, leading to greater heat generation in the shear zone. Increasing the depth of cut tends to raise the maximum temperature due to the larger volume of material being deformed and cut. Notably, for α = -6° at 250 m/min, temperatures increased from 393.75°C at Td = 0.1 mm to 452.40°C at Td = 0.2 mm. However, at some lower speeds, temperature variation with depth of cut was less pronounced, indicating possible heat dissipation effects. The tool rake angle had a significant impact on the temperature distribution: Positive rake angle (15°) consistently resulted in lower temperatures. Neutral rake angle (0°) showed moderate temperatures. Negative rake angle (-6°) produced the highest temperatures under almost all cutting conditions. This can be explained by the increased friction and resistance to cutting at negative rake angles, leading to greater heat generation. Positive rake angles favour lower cutting temperatures, supporting longer tool life and improved surface finish. High cutting speeds and negative rake angles should be carefully managed to avoid excessive thermal loading, which can accelerate tool wear. Depth of cut has a complex influence but generally, higher depths contribute to higher temperature due to larger material removal rates.

From the table 3.4 we have to know The maximum shear stress generally increases slightly with increasing cutting speed at all rake angles and depths of cut. For example, at α = 15° and Td = 0.5 mm, shear stress rises from 139.10 MPa at 50 m/min to 153.01 MPa at 250 m/min. This is attributed to higher strain rates at greater speeds, causing elevated stresses in the shear zone. Effect of Depth of Cut (Td):Shear stress increases significantly with larger depths of cut for most cases. For example, at α = -6° and 250 m/min, the shear stress goes from 159.79 MPa (Td=0.1 mm) to 195.29 MPa (Td=0.5 mm).This trend reflects the higher resistance to deformation as more material is being sheared. Negative rake angles (-6°) generally resulted in the highest shear stresses among all conditions. At a cutting speed of 250 m/min and Td=0.5 mm:α = 15° → τmax = 153.01 MPa,α = 0° → τmax = 189.70 MPa,α = -6° → τmax = 195.29 MPa. Negative rake angles increase cutting forces and hence result in higher stress generation. Positive rake angles (15°) consistently show lower shear stresses, which is favourable for tool life. Negative rake angles intensify stress concentration, risking faster tool wear or potential material failure at high cutting conditions. At higher cutting speeds and larger depths of cut,

the machining zone undergoes greater shear loads, suggesting the need for tool material optimization under aggressive cutting conditions.
From table 3.5 we have to know The Von Mises stress generally increases with higher cutting speeds across most tool rake angles and depths of cut. For instance, at α = 15° and Td = 0.5 mm, the stress increases from 342.97 MPa (50 m/min) to 374.16 MPa (250 m/min).The increase is due to higher strain rates and thermal effects induced by faster cutting. Effect of Depth of Cut (Td): Increasing depth of cut generally results in a higher Von Mises stress, especially noticeable at low rake angles. For example, at α = 0° and V = 250 m/min: Td = 0.1 mm → σeq = 382.19 MPa. Td = 0.5 mm → σeq = 391.46 MPa. Deeper cuts introduce more material resistance, resulting in greater internal stresses. Effect of Rake Angle (α): Negative rake angles (-6°) exhibit the highest Von Mises stresses compared to 0° and 15°.At V = 250 m/min and Td = 0.5 mm: α = 15° → 374.16 MPa, α = 0° → 391.46 MPa, α = -6° → 394.58 MPa. Negative rake angles increase the cutting force and plastic deformation in the material, which escalates the stress concentration. Positive rake angles (15°) tend to produce lower Von Mises stresses, making them better for smoother cutting and improved tool life. Stress increases are more pronounced at higher speeds and higher depths of cut, suggesting that careful parameter selection is necessary to prevent tool failure. Negative rake angle configurations, while sometimes improving cutting stability, lead to higher stress build-up, implying a trade-off between stability and tool wear.

3.3 Regression Analysis

Case 1. Temperature

Table 3.6. Temperature corresponds to depth of cut = 0.1 mm

V (m/min)	50	150	250	50	150	250	50	150	250
α (degree)	15	15	15	0	0	0	-6	-6	-6
T (^{0}C)	292.96	299.01	308.79	344.57	356.34	365.84	372.14	381.26	393.75

Temperature vs Rake Angle

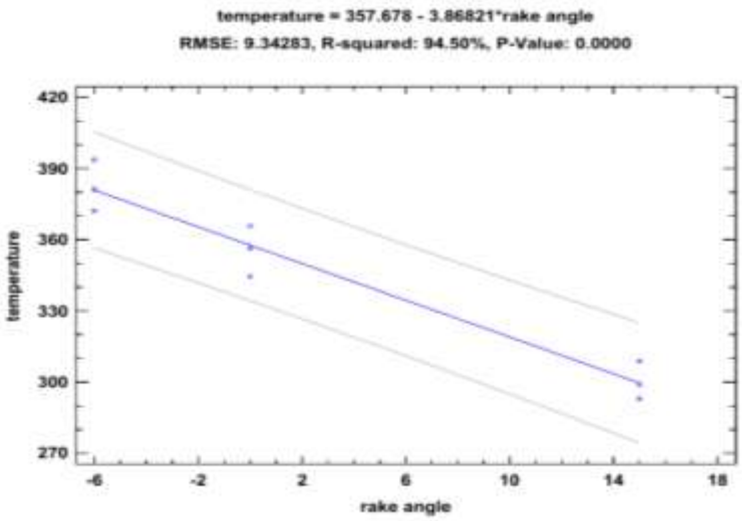

Figure 3.16. Regression analysis of temperature vs rake angle at cutting speed 50 m/min

Equation (1): Temperature = 357.678 – 3.86821 × Rake Angle

RMSE: 9.34283R² (Coefficient of Determination): 94.50% and P-Value: 0.0000
This figure illustrates the relationship between the rake angle and the cutting temperature at a cutting speed of 50 m/min. A strong negative linear relationship is observed, where the temperature decreases with an increase in rake angle. By Shear Plane Mechanics (Merchant’s Theory):A higher rake angle leads to a smaller shear plane angle, reducing the shear deformation zone. Less deformation means less energy converted into heat, thereby lowering cutting temperature. Positive rake angles facilitate smoother chip flow over the rake face of the tool. This reduces friction between the chip and the tool, which is a primary source of heat generation in metal cutting as the rake angle increases, cutting forces

decrease due to reduced resistance to chip formation. Lower cutting forces correlate with reduced mechanical work, leading to lower heat generation. Higher rake angles reduce the contact area between tool and chip, decreasing the frictional heat. The high R^2 value (94.50%) indicates that the model explains a very high proportion of the variability in temperature. The low RMSE shows good model accuracy, and the P-value confirms the regression is statistically highly significant.

Temperature vs Cutting Speed

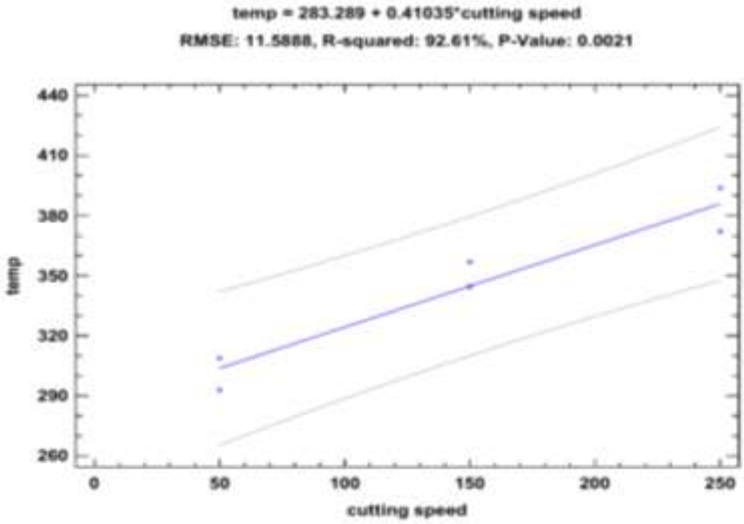

Figure 3.17. Regression analysis of temperature vs cutting speed at rake angle 15°

Equation (2): Temperature = 283.289 + 0.41035 × Cutting Speed

RMSE: 11.5888R^2 (R-squared): 92.61%. and P-Value: 0.0021

This regression analysis shows a strong linear relationship between cutting speed and temperature at a rake angle of 15°. The positive coefficient indicates that as cutting speed increases, temperature also increases. The high R^2 value (92.61%) confirms that the cutting speed explains a significant proportion of the variation in temperature, making the model reliable. The P-value (<0.05) shows statistical significance. Higher cutting speed means more mechanical energy is applied per unit time. Most of this energy converts to heat due to plastic deformation and friction. Therefore, temperature increases proportionally with cutting speed at high speeds, the chip and tool interface are exposed to friction for a shorter time. But because heat is generated faster than it can be dissipated, localized temperatures rise .a t higher speeds, the tool–chip interface becomes the dominant source of heat. Frictional heating increases rapidly with speed, adding to the temperature rise. Materials have limited time to conduct heat away due to the short tool–work contact. This results in thermal accumulation in the cutting zone**.**

Case 2. Maximum Shear Stress

Table 3.7. Maximum shear stress at depth of cut = 0.1 mm

V (m/min)	50	150	250	50	150	250	50	150	250
α (degree)	15	15	15	0	0	0	-6	-6	-6
Ʈ (MPa)	133.25	138.85	139.64	158.86	159.05	159.62	164.62	167.31	169.79

Maximum Shear Stress vs Rake Angle

Industrial Engineering Journal
ISSN: 0970-2555
Volume : 54, Issue 5, No.4, May : 2025

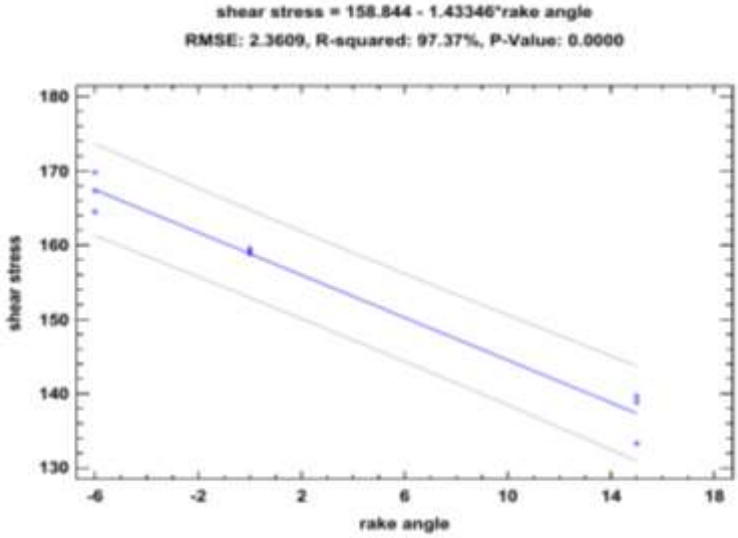

Figure 3.18. Regression analysis of maximum shear stress vs rake angle at cutting speed 50 m/min

Equation (3): Max. Shear Stress = 158.844 - 1.43346 × Rake Angle

RMSE: 2.3609R-squared**:** 97.37%,P-Value**:** 0.0000

Trend is that the negative coefficient (-1.43346) indicates that as the rake angle increases**,** the shear stress decreases. For every 1-unit increase in rake angle, shear stress decreases by approximately 1.43 units**.** Shear Stress Decreases with Increasing Rake Angle due to the Reduced Shear Plane Angle**.** a larger rake angle means the cutting edge is more "open." This reduces the shear plane angle**,** lowering resistance to chip flow and thus reducing the required shear force. Higher rake angles reduce friction between the tool and workpiece. This decreases the energy needed for shearing, thereby lowering maximum shear stress**.** The chip slides more smoothly along the rake face. Less deformation force is needed, hence less stress concentration develops in the primary shear zone. Goodness of Fit is The high R-squared (97.37%) suggests that the model explains 97.37% of the variance in shear stress, indicating a very strong linear relationship. The low RMSE (2.3609) means the model's predictions are very close to the actual data points. Statistical Significance is The P-value (0.0000) confirms that the relationship is statistically significant (well below the typical 0.05 threshold).This model shows a strong, precise, and significant negative linear relationship between rake angle and shear stress.

Maximum Shear Stress vs Cutting Speed

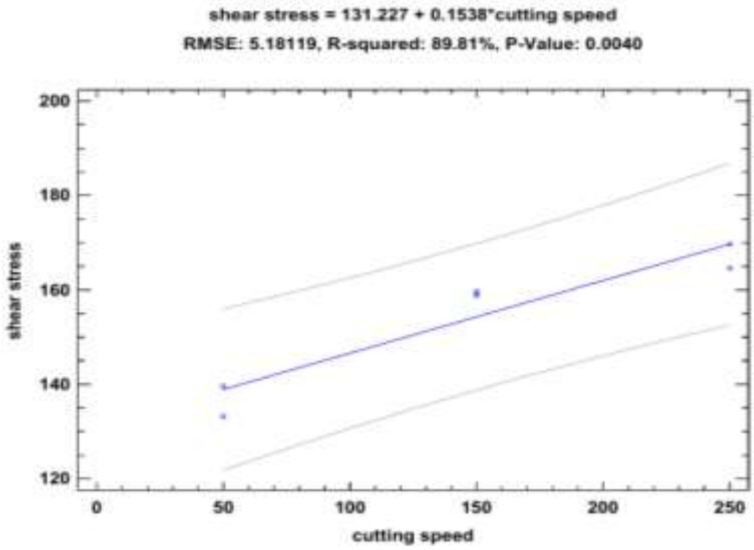

Figure 3.19. Regression analysis of maximum shear stress vs cutting speed at rake angle 15°

Equation (4): Max. Shear Stress=131.227+0.1538 × Cutting Speed

Industrial Engineering Journal
ISSN: 0970-2555
Volume : 54, Issue 5, No.4, May : 2025

This indicates that shear stress increases linearly with cutting speed, with an estimated increase of 0.1538 units in shear stress for every unit increase in cutting speed. Higher cutting speeds generating more heat, causing: Thermal softening of the material, but also increased strain rates that require higher stress for shearing. Possible work hardening effects or tool-material interaction changes at higher speeds. Tool wear might also increase at high speeds, increasing cutting forces and stress. The model's goodness of fit is shown by an R-squared value of 89.81%, meaning approximately 89.81% of the variation in shear stress can be explained by the cutting speed. The Root Mean Square Error (RMSE) is 5.18, indicating the average deviation of observed values from the predicted values. The p-value of 0.0040 suggests that the observed relationship is statistically significant at the 0.05 level.

Case 3. Von Mises Equivalent Stress

Table 3.8. Von mises equivalent stress at depth of cut = 0.1 mm

V (m/min)	50	150	250	50	150	250	50	150	250
α (degree)	15	15	15	0	0	0	-6	-6	-6
σ (MPa)	342.38	347.26	356.01	374.54	381.83	382.19	391.08	393.62	393.24

Von Mises Equivalent Stress vs Rake Angle

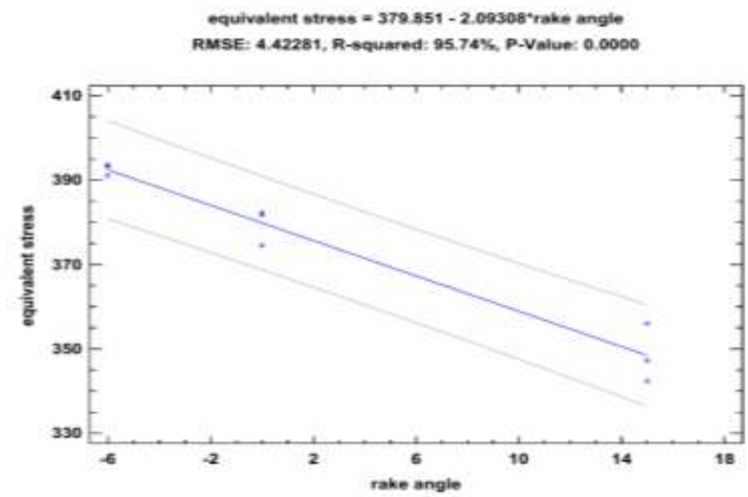

Figure 3.20. Regression analysis of von mises equivalent stress vs rake angle at cutting speed 50 m/min

Equation (5): Von Mises Equivalent Stress = 379.851 - 2.09308 × Rake Angle

RMSE: 4.42281R-squared: 95.74%. P-Value: 0.0000

Trend is The negative coefficient (-2.09308) indicates that equivalent stress decreases as rake angle increases. For every 1-unit increase in rake angle, equivalent stress decreases by ~2.09 units. A higher rake angle reduces the shear plane angle, making material deformation more efficient and lowering stress. Reduced Cutting Forces: Positive rake angles decrease cutting resistance, reducing compressive and shear stresses in the workpiece. Less Chip-Tool Friction: Higher rake angles can lead to thinner chips and reduced contact area, decreasing frictional heating and stress. Lower cutting forces at higher rake angles may reduce heat generation, preventing work hardening. A sharper rake angle promotes smoother chip flow, reducing deformation resistance. Goodness of Fit is R-squared (95.74%) shows that the model explains 95.74% of the variance in equivalent stress, indicating an exceptionally strong linear relationship. The low RMSE (4.42281) suggests high predictive accuracy. Statistical Significance is The P-value (0.0000) confirms the relationship is highly statistically significant. This model demonstrates a strong, precise, and significant negative linear relationship between rake angle and equivalent stress.

Von Mises Equivalent Stress vs Cutting Speed

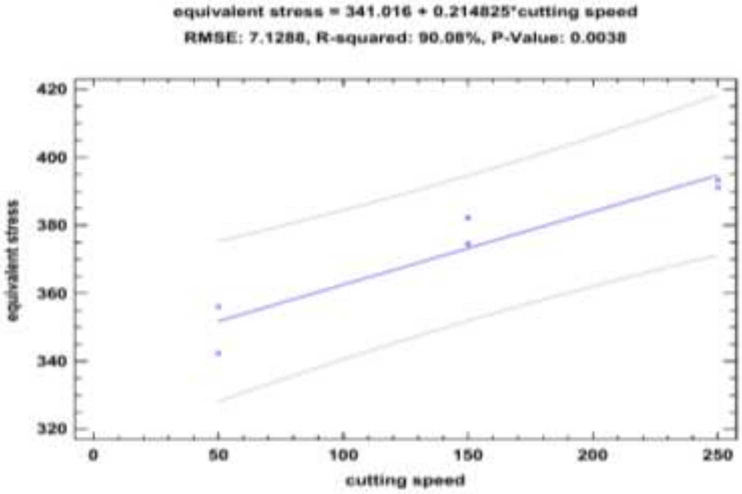

Figure 3.21. Regression analysis of von mises equivalent stress vs cutting speed at rake angle 15°

Equation (6): Von Mises Equivalent Stress = 341.016 + 0.214825 × Cutting Speed

RMSE: 7.1288R-squared: 90.08%. P-Value: 0.0000

Trend is the positive coefficient (0.214825) indicates that equivalent stress increases with cutting speed, but the effect is relatively small. For every 1-unit increase in cutting speed, equivalent stress increases by approximately 0.21 units. At higher speeds, the material deforms faster, increasing dislocation resistance and thus stress. Thermal softening (from heat generation) may be insufficient to offset this effect. Elevated speeds can intensify friction at the tool-chip interface, raising shear stress. Material-Specific Response: The workpiece (e.g., titanium, high-strength steel) may inherently exhibit positive strain-rate sensitivity. Very high speeds might localize heat, creating unstable shear bands that transiently increase stress. Goodness of Fit is the R-squared value (90.08%) shows that the model explains 90.08% of the variance in equivalent stress, indicating a strong linear relationship. The low RMSE (7.1288) suggests high predictive accuracy. Statistical Significance: The P-value (0.0038) confirms the relationship is statistically significant (well below the 0.05 threshold).This model demonstrates a statistically significant but mild positive relationship between cutting speed and equivalent stress, with excellent explanatory power.

3.4 Optimization

The goal of this study is to determine the optimal cutting parameters rake angle (α), cutting speed (V), and depth of cut (Td) that minimize the cutting temperature during turning of Aluminium 6061-T6. Lower cutting temperatures are desired to reduce thermal stresses, extend tool life, and improve surface integrity of the machined part. The temperature distribution table(table 3.3)was constructed using 27 combinations of cutting parameters, each representing a unique experimental or simulated condition. The corresponding cutting temperature values were either obtained through FEA (ANSYS Workbench) simulations. The table provided temperature values at 3 levels of rake angle: −6°, 0°, 15°, 3 levels of cutting speed: 50, 150, 250 m/min and 3 levels of depth of cut: 0.1, 0.2, 0.5 mm. This results in a 3^3 full factorial design and Total data points = 3 × 3 × 3 = 27.This structured data allowed for Identification of nonlinear trends in how temperature responds to changes in process parameters and Development of a predictive regression model.

Industrial Engineering Journal
ISSN: 0970-2555
Volume : 54, Issue 5, No.4, May : 2025

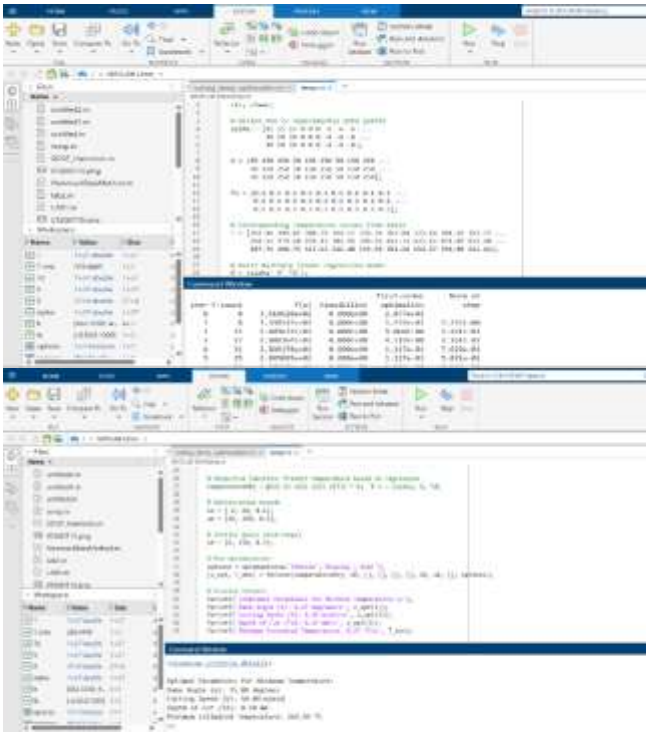

Figure 3.22. Optimization of cutting parameters and temperature in MATLAB

The optimal parameters for minimum temperature were obtained as: Rake Angle (α): 15.00 degrees, Cutting Speed (V): 50.00 m/min, Depth of Cut (Td): 0.50 mm, Minimum Estimated Temperature: 269.44 °C. These values were found by minimizing the regression-based temperature function under the given bounds. The optimization achieved convergence successfully. The result suggests that a high rake angle (15°), low cutting speed (50 m/min), and maximum depth of cut (0.5 mm) combination is most effective in reducing thermal load. This agrees with machining theory, where: a higher rake angle reduces cutting force and heat generation. Lower speeds reduce frictional heating. Deeper cuts distribute heat over a larger volume. Increasing rake angle generally reduces temperature, due to smoother chip flow and less plastic deformation. Higher cutting speeds significantly increase temperature due to more frictional heat and less time for heat dissipation. Depth of cut has a nonlinear impact; however, higher depth values can spread heat across a larger cutting zone, mitigating localized temperature rise.

IV. Conclusion

This study integrated thermal stress analysis, regression modelling, and optimization to enhance the turning of Aluminium 6061-T6, focusing on minimizing cutting temperature and associated thermal effects. Finite Element Analysis (FEA) using ANSYS Workbench revealed that maximum temperatures are concentrated in the primary shear zone and tool–workpiece interface, significantly influenced by cutting speed, rake angle, and depth of cut. Cutting speed was the most dominant factor, increasing temperature due to elevated friction and reduced heat dissipation, while a positive rake angle (15°) improved chip flow and reduced heat generation. Depth of cut (0.50 mm) showed a mixed effect, helping disperse heat but increasing mechanical load. A multiple linear regression model developed using STATGRAPHICS and MATLAB established a predictive relationship between rake angle (α), cutting speed (V), depth of cut (Td), and cutting temperature. Validated for accuracy, the model was employed as an objective function in MATLAB’s minion optimizer, yielding optimal parameters: α = 15.00°, V = 50.00 m/min, Td = 0.50 mm, with a minimum predicted cutting temperature of 269.44 °C. These settings effectively reduced thermal stress, minimized tool wear, and improved surface quality. The study confirmed a strong correlation between high cutting temperatures and increased tool wear (including flank wear and built-up edge formation), negatively impacting

Industrial Engineering Journal
ISSN: 0970-2555
Volume : 54, Issue 5, No.4, May : 2025

surface finish and fatigue strength. Overall, the integrated approach, combining ANSYS simulation, STATGRAPHICS modelling, and MATLAB optimization, offers a predictive, cost-effective, and sustainable solution aligned with Industry 4.0 practices, promoting improved reliability, reduced experimentation, lower energy consumption, and extended tool life. The methodology is adaptable to other alloys and machining conditions, contributing to advanced thermal management and optimization in metal cutting.

References

[1] Ali, M., Hussain, S., & Khan, R. (2021). Effect of thermal expansion on surface roughness during high-speed turning. *Journal of Materials Processing Technology*, 295, 117157.
[2] Fernández, E., Martín, P., & Ortega, D. (2022). Intelligent manufacturing strategies using thermal models and predictive analytics. *CIRP Journal of Manufacturing Science and Technology*, 38, 22–31.
[3] Gupta, A., Mehta, R., & Sharma, S. (2022). Integration of simulation and optimization for sustainable turning processes. *Procedia CIRP*, 104, 56–61.
[4] Kumar, S., Verma, R., & Yadav, R. (2019). Thermal analysis in metal cutting: An overview. *International Journal of Advanced Manufacturing Technology*, 105(3), 1201–1215.
[5] Liu, Y., Gao, J., & Wang, X. (2021). Optimization of cutting parameters to reduce thermal stresses in dry turning. *Precision Engineering*, 68, 45–53.
[6] Narayan, P., & Bhat, S. (2016). Influence of cutting temperature on tool wear and surface finish in aluminum machining. *International Journal of Machine Tools and Manufacture*, 102, 32–40.
[7] Patel, H., & Rao, P. N. (2017). Statistical modeling of cutting forces and temperature in turning Aluminum 6061-T6. *Measurement*, 111, 186–195.
[8] Rahman, M., Lim, Y., & Tan, C. (2021). Energy-efficient machining through simulation-based optimization. *Journal of Cleaner Production*, 293, 126199.
[9] Singh, D., Sharma, A., & Kumar, M. (2018). Thermal sensitivity and machinability of Aluminum 6061-T6. *Materials Today: Proceedings*, 5(2), 689–694.
[10] Torres, A., & Li, L. (2019). Advances in FEA modeling of thermal behavior in cutting: A review. *Applied Thermal Engineering*, 157, 113733.
[11] Wang, J., Liu, F., & Zhang, L. (2020). Multi-objective optimization of turning parameters using genetic algorithm. *Journal of Cleaner Production*, 276, 124131.
[12] Zhang, H., & Chen, X. (2020). Finite element modeling of temperature fields in turning using ANSYS. *Journal of Manufacturing Processes*, 58, 417–426.
[13] Zhou, Y., Tang, R., & Sun, Q. (2023). Data-driven machining: Toward real-time adaptive control. *Journal of Manufacturing Systems*, 66, 295–308.